DEFORMATION CHECKS ON THE SHAFTS OF BIG BAND SAW MACHINES – CASE B

Boycho Marinov

Institute of Mechanics, Bulgarian Academy of Sciences,
"Acad. G. Bonchev" Str., Block 4, 1113 Sofia, Bulgaria,
E-mails: boicho_marinoff@yahoo.co.uk, boicho_marinoff@imbm.bas.bg

Abstract. In this study, the influence of the spatial deformations on the upper shaft of big band saw machines is investigated. Deformation checks for the most endangered cross sections of the shaft are performed. For this purpose, an algorithm that includes analytical and numerical part has been developed. Theoretical expressions for calculating the spatial deformations are derived. These expressions are used to calculate the maximum deflections in the most endangered cross sections. The biggest values are compared with the admissible values for the respective material. Normal operation of the shaft, and therefore of the band saw machine is guaranteed if the actual values of the deformations are equal or less than the admissible values.

Keywords: deformation checks, deflections, spatial deformations, band saw machine, shafts, cross section, optimization procedures.

1. INTRODUCTION

The big band saw machines are object of study in this paper. These machines are widely used in the woodworking industry. They are used for cutting logs, prisms, thick and thin boards, shutters and more. Large static and dynamic loads arise in operating mode. These loads cause big deformations in the upper shafts. The influence of the spatial deformations of the shaft on their safe operation is analyzed in the proposed work. In this case, we can develop an algorithm to perform deformation checks on the most endangered cross sections. The aim of this work is to obtain expressions describing the full deformations of the main shaft. These expressions render an account the static and dynamic deformations of the shaft in two mutually perpendicular planes. Dependencies describing the static and dynamic deformations are obtained by the author in previous articles [1, 2, 3].

Another objective of this study is calculation of the actual values of the deflections in the most endangered cross sections. The theoretical expressions

DOI: 10.7546/EngSci.LIX.24.04.06

describing the spatial deformations are used for the numerical calculations. Finding the maximum of the function can be performed in different ways. Some of these ways are described in the second part of the article.

The final objective of this study is a deformation check of the upper shaft of the band saw machine to be performed. For this purpose the absolute or relative deflections of the shaft in the most endangered cross sections must be compared with the admissible absolute or relative deflections. Normal operation of the band saw machine is ensured if the real deflections are smaller or equal to the limit values established in the technical literature [4–8].

2. EXPOSE

2.1. Scheme of the cutting mechanism

The leading wheel of the big band saw machines can be mounted on the upper shaft in two ways. These cases are written as case (a) and case (b). In this study, we consider case (b), when leading wheel is mounted between the two bearing supports.

The scheme of the cutting mechanism is shown in Fig. 1 [1, 3, 9]. In this section, we obtain expressions for performing a deformation check on the upper

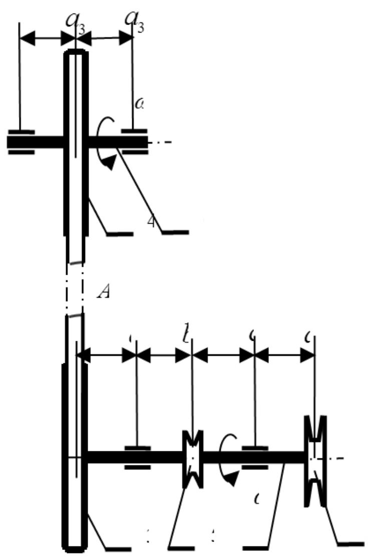

Fig. 1. Cutting mechanism

shaft when the leading wheel is mounted between the two bearing supports, i.e., case (b).

The following symbols are defined: 1-main shaft, 2 and 5-belt pulleys, 3 and 4-leading wheels, A-band saw blade, and 6-upper shaft.

2.2. Dynamic model

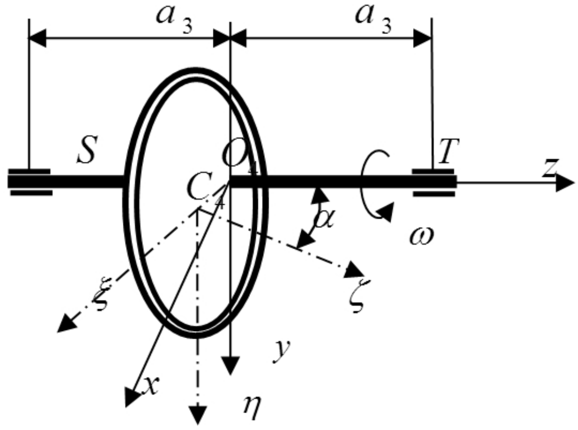

Fig. 2. Dynamic model

The dynamic model is shown in Fig. 2. The following coordinate systems are used:
fixed coordinate system O_4xyz and coordinate system $C_4\xi\eta\zeta$ whose axes are principal axes of inertia. The linear and angular deviations e and α are also shown in the figure as $e = O_4C_4$ and α is the angle between the axes ζ and z.

2.3. Deformation checks-analytical solution

The upper shaft consists of two parts – SO_4 and O_4T. Deformation checks can be performed analytically and numerically by using the following algorithm [10]:

– expressions describing the static and dynamic deformations of the shaft in two mutually perpendicular planes are used;
– the full deformations for the relevant axes are determined;
– the full deflection of the shaft for each part is calculated from known dependencies;
– the endangered cross-section of the shaft is determined. This is the section where the full deflection is the biggest. We denote this deflection with $f_{\max}$;

– the calculated value of $f_{\max}$ is used for deformation check of the shaft.

This algorithm is applied to each part.

I. Part SO_4 $0 \le z \le a_3$.

– static and dynamic deformations of the upper shaft in two mutually perpendicular planes;

$$\begin{aligned}
&y^{st}_{SO_4}(z) = \frac{1}{EJ}\left(\frac{S^{st}_y}{6}z^3 + S_1 z + T_1\right),\\
&x^{st}_{SO_4}(z) = \frac{1}{EJ}\left(\frac{S^{st}_x}{6}z^3 + S_3 z + T_3\right),\\
&y^{dyn}_{SO_4}(z,t) = (\bar{S}_1 \cos\omega_0 z + \bar{T}_1 \sin\omega_0 z + \bar{V}_1 \operatorname{ch}\omega_0 z + \bar{W}_1 \operatorname{sh}\omega_0 z)\sin\omega t,\\
&x^{dyn}_{SO_4}(z,t) = (\bar{S}_3 \cos\omega_0 z + \bar{T}_3 \sin\omega_0 z + \bar{V}_3 \operatorname{ch}\omega_0 z + \bar{W}_3 \operatorname{sh}\omega_0 z)\cos\omega t.
\end{aligned} \tag{1}$$

full deformation of the upper shaft for the relevant axes;

$$\begin{aligned}
y_{SO_4\Sigma}(z,t) &= y^{st}_{SO_4}(z) + y^{din}_{SO_4}(z,t)\\
x_{SO_4\Sigma}(z,t) &= x^{st}_{SO_4}(z) + x^{din}_{SO_4}(z,t)
\end{aligned} \tag{2}$$

– deflection of the upper shaft for part SO_4;

$$f_{SO_4}(z,t) = \sqrt{(y_{SO_4\Sigma}(z,t))^2 + (x_{SO_K\Sigma}(z,t))^2}. \tag{3}$$

This expression is transformed into the following form to obtain the dependence for calculating the full deflection of the upper shaft.

$$\begin{aligned}
&f_{O_4K}(z,t)\\
&= \sqrt{\begin{aligned}
&(y^{st}_{SO_4}(z))^2 + (x^{st}_{SO_4}(z))^2\\
&+2[y^{st}_{SO_4}(\bar{S}_1 \cos\omega_0 z + \bar{T}_1 \sin\omega_0 z + \bar{V}_1 \operatorname{ch}\omega_0 z + \bar{W}_1 \operatorname{sh}\omega_0 z)\sin\omega t]\\
&+2[x^{st}_{SO_4}(\bar{S}_3 \cos\omega_0 z + \bar{T}_3 \sin\omega_0 z + \bar{V}_3 \operatorname{ch}\omega_0 z + \bar{W}_3 \operatorname{sh}\omega_0 z)\cos\omega t]\\
&+[(\bar{S}_1 \cos\omega_0 z + \bar{T}_1 \sin\omega_0 z + \bar{V}_1 \operatorname{ch}\omega_0 z + \bar{W}_1 \operatorname{sh}\omega_0 z)\sin\omega t]^2\\
&+[(\bar{S}_3 \cos\omega_0 z + \bar{T}_3 \sin\omega_0 z + \bar{V}_3 \operatorname{ch}\omega_0 z + \bar{W}_3 \operatorname{sh}\omega_0 z)\cos\omega t]^2
\end{aligned}}\,,
\end{aligned} \tag{4}$$

II. Part O_4T $a_3 \le z \le 2a_3$ static and dynamic deformations of the upper shaft in two mutually perpendicular planes;

$$
\begin{aligned}
&y^{st}_{O_4T}(z) = \frac{1}{EJ}\left[\frac{(G^e_4 + 2F^e_4 + S^{st}_y)}{6}z^3 + \frac{[M^e_{G_4x} - (G^e_4 + 2F^e_4)a_3]}{2}z^2\right.\\
&\qquad\qquad \left. +S_2 Z + T_2\right],\\
&x^{st}_{O_4T}(z) = \frac{1}{EJ}\left(\frac{S^{st}_x}{6}z^3 + \frac{M^{st}_{R_4y}}{2} + S_4 Z + T_4\right),\\
&y^{dyn}_{O_4T}(z,t) = (\bar{S}_2\cos\omega_0 z + \bar{T}_2\sin\omega_0 z + \bar{V}_2\operatorname{ch}\omega_0 z + \bar{W}_2\operatorname{sh}\omega_0 z)\sin\omega t,\\
&x^{dyn}_{O_4T}(z,t) = (\bar{S}_4\cos\omega_0 z + \bar{T}_4\sin\omega_0 z + \bar{V}_4\operatorname{ch}\omega_0 z + \bar{W}_4\operatorname{sh}\omega_0 z)\cos\omega t.
\end{aligned}
\tag{5}
$$

full deformation of the upper shaft for the relevant axes;

$$
\begin{aligned}
y_{O_4T\Sigma}(z,t) &= y^{st}_{O_4T}(z) + y^{din}_{O_4T}(z,t)\\
x_{O_4T\Sigma}(z,t) &= x^{st}_{O_4T}(z) + x^{din}_{O_4T}(z,t)
\end{aligned}
\tag{6}
$$

full deflection of the upper shaft for part O_4T;

$$
f_{O_4T}(z,t) = \sqrt{(y_{O_4T\Sigma}(z,t))^2 + (x_{O_4T\Sigma}(z,t))^2}. \tag{7}
$$

We replace $y_{O_4T\Sigma}(z,t)$ and $x_{O_4T\Sigma}(z,t)$in the above expression with their equals and obtain the dependence for calculating the full deflection of the upper shaft.

$$
\begin{aligned}
&f_{O_4T}(z,t)\\
&= \sqrt{\begin{aligned}
&(y^{st}_{O_4T}(z))^2 + (x^{st}_{O_4T}(z))^2\\
&+2[y^{st}_{O_4T}(\bar{S}_2\cos\omega_0 z + \bar{T}_2\sin\omega_0 z + \bar{V}_2\operatorname{ch}\omega_0 z + \bar{W}_2\operatorname{sh}\omega_0 z)\sin\omega t]\\
&+2[x^{st}_{O_4T}(\bar{S}_4\cos\omega_0 z + \bar{T}_4\sin\omega_0 z + \bar{V}_4\operatorname{ch}\omega_0 z + \bar{W}_4\operatorname{sh}\omega_0 z)\cos\omega t]\\
&+[(\bar{S}_2\cos\omega_0 z + \bar{T}_2\sin\omega_0 z + \bar{V}_2\operatorname{ch}\omega_0 z + \bar{W}_2\operatorname{sh}\omega_0 z)\sin\omega t]^2\\
&+[(\bar{S}_4\cos\omega_0 z + \bar{T}_4\sin\omega_0 z + \bar{V}_4\operatorname{ch}\omega_0 z + \bar{W}_4\operatorname{sh}\omega_0 z)\cos\omega t]^2
\end{aligned}}\ ,
\end{aligned}
\tag{8}
$$

The following symbols are used in the above expressions:

S_i, T_i, $(i = 1, 2)$ are constants of integration. They take part in the expressions for $y^{st}_{SO_4}$ and $y^{st}_{O_4T}$ and can be calculated from the following dependencies:

$$S_1 = -\frac{a_3[G_4^e + 2F_4^e + 8S_y^{st})a_3 + 3M_{G_4x}^e]}{12}, \qquad T_1 = 0,$$
$$S_2 = -\frac{a_3[5G_4^e + 10F_4^e - 8S_y^{st})a_3 - 15M_{G_4x}^e]}{12}, \tag{9}$$
$$T_2 = -\frac{a_3^2[3M_{G_4x}^e - (G_4^e + 2F_4^e)a_3]}{6}.$$

S_j, T_j, $(j = 3, 4)$ are constants of integration. They take part in the expressions for $x_{SO_4}^{st}$ and $x_{O_4T}^{st}$ and can be calculated from the following dependencies:

$$\begin{aligned} S_3 &= \frac{-3a_3(3M_{R_4y}^{st} + 8a_3S_x^{st}}{12}, \quad T_3 = 0, \\ S_4 &= \frac{-3a_3(15M_{R_4y}^{st} + 8a_3S_x^{st}}{12}, \quad T_4 = \frac{M_{R_4y}^{st}a_3^2}{2}. \end{aligned} \tag{10}$$

G_4^e, F_4^e, $M_{G_4x}^e$ and $M_{R_4y}^{st}$ are static forces and moments. They can be calculated from the dependences (11) written below.

$$\begin{aligned} &M_{G_4x}^e = m_4 g e \sin\alpha, \quad M_{R_4y}^{st} = \frac{1}{2}\left(\frac{mK_{\Delta(\lambda)}bHu}{V} + R_\Sigma\right) r_4 \cos\alpha, \\ &G_4^e = m_4 g, \quad F_4^e = 1.5N_c/V, \end{aligned} \tag{11}$$

where $m+4$ and r_4 are the mass and the radius of the leading wheel 4 and g is the acceleration of gravity. R_Σ is the total resistance force. H is the thickness of the workpiece or sawing height, u is the feeding speed, b is the width of the cutter. m is a coefficient $(0 \le m \le 1)$. N is the cutting power and V is the cutting speed. $K_{\Delta(\lambda)}$ is the specific work of the cutting [11].

$$K_\Delta = k + \frac{a_\rho p}{u_{z\Delta}} + \frac{\alpha_\Delta H}{b}, \quad K_\lambda = k + \frac{a_\rho ps}{bu_{z\lambda}} + \frac{\alpha_\lambda H}{b}. \tag{12}$$

The symbol $\alpha_{\Delta(\lambda)}$ is the friction intensity of the shavings on the sawing walls, as α_Δ is used for swage-set teeth and α_λ is used for part-set teeth $(\alpha_\lambda = 1.25\alpha_\Delta)$.

a_ρ is a coefficient of the blunt teeth, $(1.4 \le a_\rho \le 2.8)$. s is the thickness of the band saw blades. k is the fictitious pressure on the front side of the teeth and p is the fictitious specific force on the back side of the teeth. The feeding of one tooth is marked with $u_{z\Delta}$, $u_{z\lambda}$.

S_x^{st} and S_y^{st} are static reactions. They are caused by static forces and moments participating in the above expressions and can be calculated from the following dependencies:

$$
\begin{aligned}
S_x^{st} &= -\frac{r_4}{4a_3}\left(\frac{mK_{\Delta(\lambda)}bHu}{V} + R_\Sigma\right)\cos\alpha, \\
S_y^{st} &= -\frac{m_4 g}{2a_3}(e\sin\alpha + a_3) - \frac{1.5N_c}{V}.
\end{aligned}
\tag{13}
$$

$\bar{S}_i$, $\bar{T}_i$, $\bar{V}_i$, $\bar{W}_i$, $(i = 1, 2)$ are constants of integration. They take part in the expressions that describe the deformations of the shaft by the dynamic loads and can be calculated from the following expressions:

$$
\bar{S}_i = \frac{\Delta_{\bar{S}_i}}{\Delta_P},\ \bar{T}_i = \frac{\Delta_{\bar{T}_i}}{\Delta_P},\ \bar{V}_i = \frac{\Delta_{\bar{V}_i}}{\Delta_P},\ \bar{W}_i = \frac{\Delta_{\bar{W}_i}}{\Delta_P},\ (i = 1, 2),
\tag{14}
$$

where $\Delta_P = \det P$ is the determinant of the matrix $\mathbf{P}$. This determinant is non-zero, because otherwise the mechanical system will operate in resonance mode and it has the following form:

$$
\mathbf{P} =
\tag{15}
$$

$$
\begin{bmatrix}
1 & 0 & 1 & 0 & 0 & 0 & 0 & 0 \\
0 & -1 & 0 & 1 & 0 & 0 & 0 & 0 \\
-1 & 0 & 1 & 0 & 0 & 0 & 0 & 0 \\
\cos\omega_0 a_3 & \sin\omega_0 a_3 & \operatorname{ch}\omega_0 a_3 & \operatorname{sh}\omega_0 a_3 & -\cos\omega_0 a_3 & -\sin\omega_0 a_3 & -\operatorname{ch}\omega_0 a_3 & -\operatorname{sh}\omega_0 a_3 \\
-\sin\omega_0 a_3 & \cos\omega_0 a_3 & \operatorname{sh}\omega_0 a_3 & \operatorname{ch}\omega_0 a_3 & \sin\omega_0 a_3 & -\cos\omega_0 a_3 & -\operatorname{sh}\omega_0 a_3 & -\operatorname{ch}\omega_0 a_3 \\
0 & 0 & 0 & 0 & \cos 2\omega_0 a_3 & \sin 2\omega_0 a_3 & \operatorname{ch} 2\omega_0 a_3 & \operatorname{sh} 2\omega_0 a_3 \\
0 & 0 & 0 & 0 & -\cos 2\omega_0 a_3 & -\sin 2\omega_0 a_3 & \operatorname{ch} 2\omega_0 a_3 & \operatorname{sh} 2\omega_0 a_3 \\
0 & 0 & 0 & 0 & -\sin 2\omega_0 a_3 & \cos 2\omega_0 a_3 & -\operatorname{sh} 2\omega_0 a_3 & -\operatorname{ch} 2\omega_0 a_3
\end{bmatrix}
$$

The determinants $\Delta_{\bar{S}_i}$, $\Delta_{\bar{T}_i}$, $\Delta_{\bar{V}_i}$ and $\Delta_{\bar{W}_i}$ $(i = 1, 2)$ are determinants of the matrices formed by the matrix $\mathbf{P}$ in which the corresponding columns are replaced by the column vector $\mathbf{p}$ as follows:

$\Delta_{\bar{S}_i}$ $(i = 1, 2)$ – the first or fifth column of the matrix $\mathbf{P}$,
$\Delta_{\bar{T}_i}$ $(i = 1, 2)$ – the second or sixth column of the matrix $\mathbf{P}$,
$\Delta_{\bar{V}_i}$ $(i = 1, 2)$ – the third or seventh column of the matrix $\mathbf{P}$,
$\Delta_{\bar{W}_i}$ $(i = 1, 2)$ – the fourth or eighth column of the matrix $\mathbf{P}$.

The column-vector $\mathbf{p}$ has the following form:

$$
\mathbf{p} = \begin{bmatrix} 0 & \dfrac{S_{bm}}{EJ\omega_0^3} & 0 & 0 & 0 & 0 & 0 & \dfrac{T_{bm}}{EJ\omega_0^3} \end{bmatrix}^T.
\tag{16}
$$

where the amplitudes S_{bm} and T_{bm} are calculated from the following dependencies:

$$
\begin{aligned}
S_{bm} &= -\frac{1}{4a_3}\left(\frac{mK_{\Delta(\lambda)}bHu}{V} + R_\Sigma\right) e\cos\alpha \\
&\quad + \frac{\omega^2}{2}\left[\frac{1}{a_3}\left(J_\xi - J_\zeta - m_4e^2\right)\sin\alpha - m_4e\right]\cos\alpha, \\
T_{bm} &= \frac{1}{4a_3}\left(\frac{mK_{\Delta(\lambda)}bHu}{V} + R_\Sigma\right) e\cos\alpha \\
&\quad - \frac{\omega^2}{2}\left[\frac{1}{a_3}\left(J_\xi - J_\zeta - m_4e^2\right)\sin\alpha + m_4e\right]\cos\alpha.
\end{aligned}
\tag{17}
$$

ω_0 is parameter, ($\omega_0^4 = A_{ms}\rho\omega^2/EJ$), [12, 13]. In this expression E is the modulus of elasticity, $J = J_x = J_y$ is the axial moment of inertia, A_{ms} is the cross-sectional area of the shaft, ρ is the density of the material. J_ξ and J_ζ are the mass moments of inertia of the leading wheel.

$\bar{S}_j$, $\bar{T}_j$, $\bar{V}_j$, $\bar{W}_j$, ($j = 3, 4$) are constants of integration. They can be calculated from the following expressions:

$$
\bar{S}_j = \frac{\Delta_{\bar{S}_i}}{\Delta_Q},\ \bar{T}_j = \frac{\Delta_{\bar{T}_i}}{\Delta_Q},\ \bar{V}_j = \frac{\Delta_{\bar{V}_i}}{\Delta_Q},\ \bar{W}_j = \frac{\Delta_{\bar{W}_i}}{\Delta_Q},\ (i = 1, 2), \tag{18}
$$

where $\Delta_Q = \det Q$ is the determinant of the basic matrix $\mathbf{Q}$ of the linear system. This matrix has the following form:

$$
\mathbf{Q} = \tag{19}
$$

$$
\begin{bmatrix}
1 & 0 & 1 & 0 & 0 & 0 & 0 & 0 \\
-1 & 0 & 1 & 0 & 0 & 0 & 0 & 0 \\
\cos\omega_0a_3 & \sin\omega_0a_3 & \operatorname{ch}\omega_0a_3 & \operatorname{sh}\omega_0a_3 & -\cos\omega_0a_3 & -\sin\omega_0a_3 & -\operatorname{ch}\omega_0a_3 & -\operatorname{sh}\omega_0a_3 \\
-\sin\omega_0a_3 & \cos\omega_0a_3 & \operatorname{sh}\omega_0a_3 & \operatorname{ch}\omega_0a_3 & \sin\omega_0a_3 & -\cos\omega_0a_3 & -\operatorname{sh}\omega_0a_3 & -\operatorname{ch}\omega_0a_3 \\
-\sin\omega_0a_3 & \cos\omega_0a_3 & -\operatorname{sh}\omega_0a_3 & -\operatorname{ch}\omega_0a_3 & \sin\omega_0a_3 & -\cos\omega_0a_3 & \operatorname{sh}\omega_0a_3 & \operatorname{ch}\omega_0a_3 \\
\cos\omega_0a_3 & \sin\omega_0a_3 & -\operatorname{ch}\omega_0a_3 & -\operatorname{sh}\omega_0a_3 & -\cos\omega_0a_3 & -\sin\omega_0a_3 & \operatorname{ch}\omega_0a_3 & \operatorname{sh}\omega_0a_3 \\
0 & 0 & 0 & 0 & \cos 2\omega_0a_3 & \sin 2\omega_0a_3 & \operatorname{ch} 2\omega_0a_3 & 2\operatorname{sh}\omega_0a_3 \\
0 & 0 & 0 & 0 & -\cos 2\omega_0a_3 & -\sin 2\omega_0a_3 & \operatorname{ch} 2\omega_0a_3 & \operatorname{sh} 3\omega_0a_3
\end{bmatrix}
$$

The determinants $\Delta_{\bar{S}_j}$, $\Delta_{\bar{T}_j}$, $\Delta_{\bar{V}_j}$ and $\Delta_{\bar{W}_j}$ ($j = 3, 4$) are determinants of the matrices formed by the matrix $\mathbf{Q}$ in which the corresponding columns are replaced by the column vector $\mathbf{q}$ in the same way as the determinants in expressions (15).

The column-vector $\mathbf{q}$ has the following form:

$$
\mathbf{q} = \begin{bmatrix} 0 & 0 & 0 & 0 & \dfrac{m_4\omega^2 e\cos\alpha}{EJ\omega_0^3} & \dfrac{M_{bm}}{EJ\omega_0^2} & 0 & 0 \end{bmatrix}^T. \tag{20}
$$

Amplitude

$$M_{bm} = \frac{1}{2}\left[\left(\frac{mK_{\Delta(\lambda)}bHu}{V} + R_\Sigma\right) e\cos\alpha - \omega^2\left(J_\xi - J_\zeta - m_4e^2\right)\sin 2\alpha\right].$$

2.3. Deformation checks – numerical solution

We use the obtained theoretical expressions to perform deformation checks on the upper shaft. The spatial deformations of the whole shaft can be obtained using expressions (4) and (8). These deformations are shown in Fig. 3.

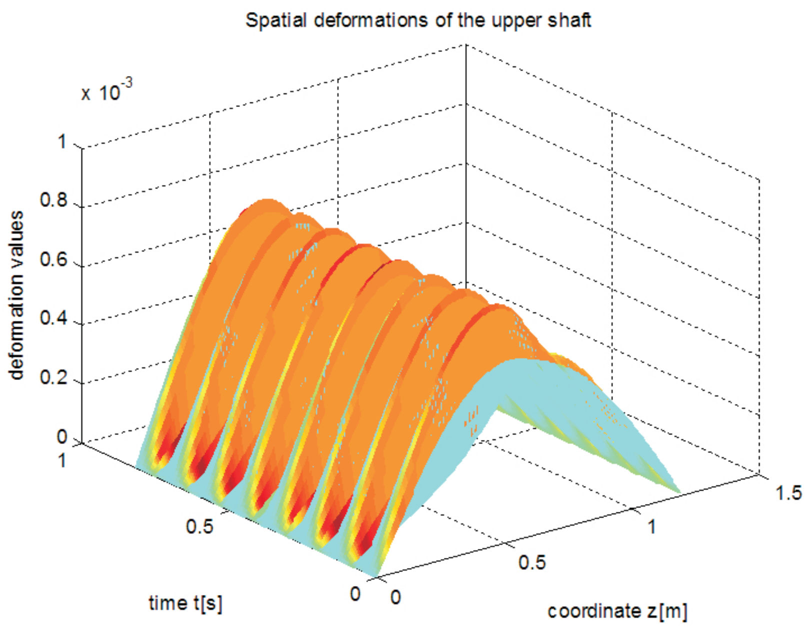

Fig. 3. Spatial deformations for the two parts of the shaft

The following initial data are used [9, 11, 14-18]:
$\omega = 56$ [s^{-1}], $\omega_0 = 0.6971$ [1/m], $e = 0.001$ [m], $\alpha = 0.01744$ [rad], $a_2 = 0.4$ [m], $b_2 = 0.8$ [m], $g = 9.81$ [m/s^2], $m_4 = 810$ [kg], $J_\xi = 171$ [kg m^2], $J_\zeta = 336$ [kg m^2], $J_x = J_y = J = 321.8\,e{-}008$ [m^4], $A_{ms} = 63.585\,e{-}004$ [m^2], $N_c = 43.4$ [kW], $V = 45$ [m/s], $u = 0.5$ [m/s], $r_4 = 0.8$ [m], $s = 1.47$ [mm], b = 2.5[mm], $p = 9220$ [N/m], $k = 35 \times 10^6$ [Pa], $\alpha_\lambda = 245 \times 10^3$ [Pa], $\alpha_\Delta = 196 \times 10^3$ [Pa], $m = 0.5$, $H = 0.42$ [m], $u = 0.5$ [m/s], $u_{z\Delta} = 2.5$ [mm], $K_\Delta = 80 \times 10^6$ [J/m^3],

$R_\Sigma = 2400$ [N], $\rho = 7850$ [kg/m^3], $F_4^e = 1450$ [N], $R_\Sigma = 2400$ [N], $P_u = 2850$ [N], $G = 7946$ [N], $E = 2.06\,e + 011$ [Pa].

Obviously, the most endangered cross-section is situated in the part SO_4. Figure 4 shows the spatial deformations of the shaft for this part.

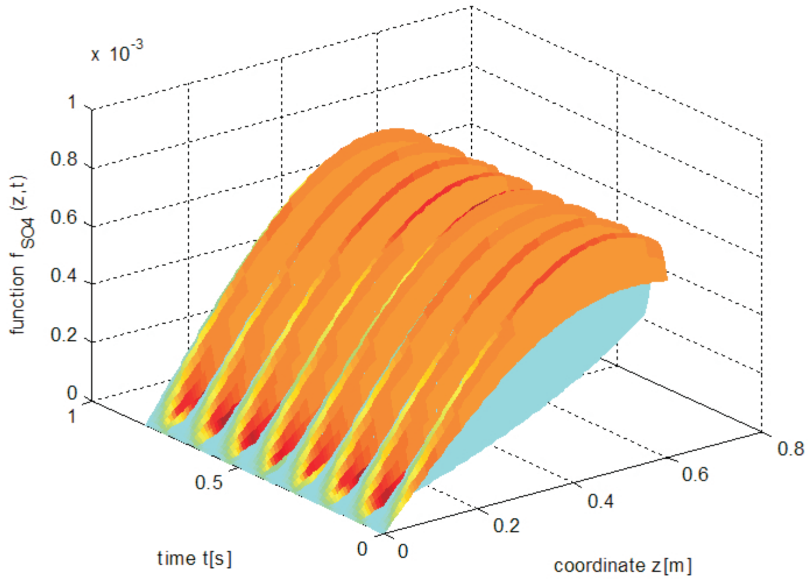

Fig. 4. Spatial deformation of the upper shaft – part SO_4

We use the part of the algorithm for numerical solution presented in section 2.3. Obviously, the most endangered cross-section is situated where $z = 0.5$ [m]. We denote $f_{SO_4}(0.5, t) = {}_{\max}f_{SO_4}$. We need to build a plane diagram for this cross section. For this reason, we write expression (4) as follows.

$$
\begin{aligned}
&f_{SO_4}(z,t)\\
&= \sqrt{\begin{aligned}&(y^{st}_{SO_4}(z))^2 + (x^{st}_{SO_4}(z))^2\\
&+2[(y^{st}_{SO_4}(0.5))(\bar{S}_1\cos(\omega_0 0.5) + \bar{T}_1\sin(\omega_0 0.5) + \bar{V}_1\,\mathrm{ch}(\omega_0 0.5)\\
&+\bar{W}_1(\omega_0 0.5))\sin\omega t] + 2[(x^{st}_{SO_4}(0.5))(\bar{S}_3\cos(\omega_0 0.5) + \bar{T}_3\sin(\omega_0 0.5)\\
&+\bar{V}_3\,\mathrm{ch}(\omega_0 0.5) + \bar{W}_3\,\mathrm{sh}(\omega_0 0.5))\cos\omega t] + [(\bar{S}_1\cos(\omega_0 0.5)\\
&+\bar{T}_1\sin(\omega_0 0.5) + \bar{V}_1\,\mathrm{ch}(\omega_0 0.5) + \bar{W}_1\,\mathrm{sh}(\omega_0 0.5))\sin\omega t]^2\\
&+[(\bar{S}_3\cos(\omega_0 0.5) + \bar{T}_3\sin(\omega_0 0.5) + \bar{V}_3\,\mathrm{ch}(\omega_0 0.5)\\
&+\bar{W}_3\,\mathrm{sh}(\omega_0 0.5))\cos\omega t]^2\end{aligned}}
\end{aligned}
\tag{21}
$$

$$y_{SO_4}^{st}(0.5) = \frac{1}{EJ}\left(\frac{S_y^{st}}{6}0.5^3 + S_1 0.5 + T_1\right),$$

$$x_{SO_4}^{st}(0.5) = \frac{1}{EJ}\left(\frac{S_x^{st}}{6}0.5^3 + S_3 0.5 + T_3\right).$$

Using this expression, we draw the diagram of the function $f_{SO_4}(0.5, t)$, which is shown in Fig. 5.

The maximum value of the deformation expression must be determined by calculating the values of the function in the area of the local maximum or by using optimization procedures to find the maximum of the function.

a) first way: calculation of the maximum values of the function.

Figure 5 shows the diagram of the function $f_{SO_4}(0.5, t)$.

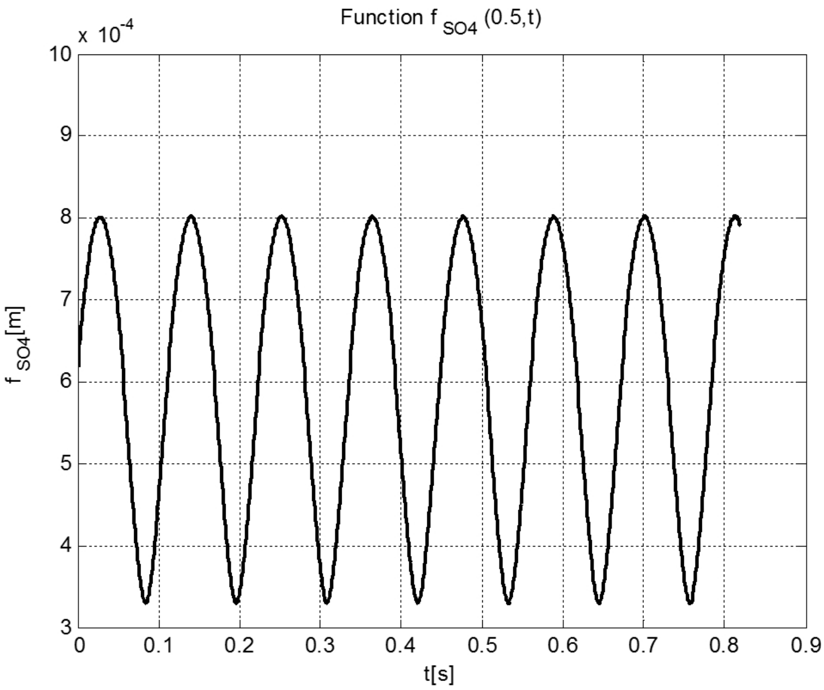

Fig. 5. Diagram of the function $f_{SO_4}(0.5, t)$

$$f_{SO_4} = 1.0\mathrm{e}-003 *$$

$$\left[\begin{array}{lllll}
\text{Columns 1 through 5} & & & & \\
0.46065608 & 0.47360947 & 0.48670604 & 0.49989491 & 0.51312900 \\
\text{Columns 6 through 10} & & & & \\
0.52636481 & 0.53956208 & 0.55268352 & 0.56569459 & 0.57856320 \\
. & & & & \\
. & & & & \\
\text{Columns 41 through 45} & & & & \\
0.80191947 & 0.80157025 & 0.80070052 & 0.79931130 & 0.79740420 \\
. & & & & \\
. & & & & \\
\text{Columns 91 through 95} & & & & \\
0.35090300 & 0.34443599 & 0.33903971 & 0.33478338 & 0.33172460 \\
\text{Columns 96 through 100} & & & & \\
0.32990646 & 0.32935531 & 0.33007926 & 0.33206770 & 0.33529194
\end{array}\right]$$

This diagram is drawn using the expression (21). We can assume that the first local maximum appears in the interval $0.1 \leq t \leq 0.2$ [s]. The values of the function $f_{SO_4}(0.5, t)$ are written as a matrix shown above.

Precise calculations show the exact value of the maximum deflection: ${}_{\max}f_{SO_4} = 0.80191947\ 068912\, e - 003$ [m]. This value should be used to perform a deformation check of the shaft, if it is the largest measured value. For other calculations, we can use the following abbreviated value ${}_{\max}f_{SO_4} = 0.80191947\, e - 003$ [m].

b) second way: use of optimization procedures for finding the maximum of the function.

We use the optimization procedure *fmincom* to determine ${}_{\max}f_{SO_4}$ [19, 20]. It is necessary to determine the initial approximations of the coordinates z and t, for which the function possesses a maximum value. These initial approximations are determined by Fig. 4 and Fig. 5. We define the following values: x0=[0.5 0.15]. The procedure requires the interval boundaries, in which the coordinates z and t change their values to be determined. In the present case, these intervals are: lower bounds $lb = [0\ 0]$, upper bounds $ub = [0.6\ 0.82]$.

```
function F=def1(x)
x0=[0.5 0.15];
lb=[0 0]; ub=[0.6 0.82];
ops=optimset('LargeScale','off');
```

[x,fval,exitflag,output]=fmincon(@def2,x0,[],[],[],[],lb,ub,[],ops)

$$z = 0.4995496618\,6438 \text{ [m]},\ t = 0.13965853\,928916 \text{ [s]},$$

$$_{\max}f_{SO_4} = 8.0200169018\,97315\,e - 004 \text{ [m]}.$$

exitflag = 5

output = algorithm: 'medium-scale: SQP, Quasi-Newton, line-search'

It is obvious that the calculated result for $_{\max}f_{SO_4}$ is the same as this one in the first way to find the maximum of the function. This deflection is the greatest deflection. It is denoted by $f_{\max}$ and can be used to perform a deformation check of the upper shaft. In this case, the following expressions are used [4, 5, 6]:

$$f_{\max} \leq [f], \quad f_{\max}/l_b \leq [f/l_b], \tag{22}$$

where $[f]$ is the admissible deflection and $[f/l_b]$ is the admissible relative deflection. The values of this deflection are taken from technical literature. We can choose the most appropriate value for each particular case, i.e. $[f/l_b] = a_b$. The admissible deflection can be calculated in the following way: $[f] = a_b l_b$. The distance l_b takes the same values for the different parts, i.e. for parts SO_4 and O_4T, $l_b = a_3$. The deformation conditions are satisfied if the maximum deflection $f_{\max}$ or the maximum relative deflection $f_{\max}/l_b$ are smaller or equal to the respective admissible deflections. The final expressions are shown below.

$$f_{\max} \leq a_b l_b, \quad f_{\max}/l_b \leq a_b. \tag{23}$$

3. CONCLUSION

In this study, the main purpose of the research is fulfilled, namely to perform deformation check of the upper shaft of big band saw machines. The two main ways by calculating the maximum value of the deformation expression are used. These ways are considered in section 2.4. In order to achieve the formulated purpose, the three main tasks have been solved.

a) expressions describing the full deformations of the upper shaft are obtained. These expressions render an account the static and dynamic deformations of the shaft in two mutually perpendicular planes.

b) the actual values of the deflections in the most endangered cross sections are calculated. The theoretical expressions describing the spatial deformations for the numerical calculations are used.

c) deformation check of the upper shaft for case (b) to be performed is the final task. To this end, the absolute or relative deflections of the upper shaft in the most endangered cross section is compared with the admissible absolute or relative deflections. Normal operation of the band saw machine is ensured if the real deflections are smaller or equal to the limit values established in the technical literature.

In conclusion, we can say that the obtained theoretical expressions and numerical results, as well as the proposed algorithm for deformation checks can be used in the design of other classes of woodworking machines.

REFERENCES

[1] B. Marinov, Investigation OF THE Spatial Deformations and Transverse Vibrations in Main Links of Big Band Saw Machines, *Journal of Theoretical and Applied Mechanics* (2024) **54** (1) 73–88, Print ISSN: 0861-6663, Online ISSN: 1314-8710, online: https://doi.org/10.55787/jtams.24.54.1.073.

[2] B. Marinov, Spatial deformations and transverse vibrations in the cutting mechanisms of big band saw machines: Investigation and analysis, *Global Journal of Engineering and Technology Advances* (2022) **13** (3) 96–109, ISSN: 2582-5003, online: https://doi.org/10.30574/gjeta.2022.13.3.0211.

[3] B. Marinov, *Energy Losses in Big Woodworking Machines: Analysis and Optimization*, Cambridge Scholars Publishing (2023), ISBN: 1-5275-1533-8, ISBN13: 978-1-5275-1533-8.

[4] I. Kisyov, *Strength of Materials*, State Publishing House “Technique” (1978).

[5] V. Milkov, *Strength of Materials, Part I* Offset-Printed Base at TU Varna (2008).

[6] V. Milkov, *Strength of Materials, Part II* Offset-Printed Base at TU Varna (2010).

[7] E. Hearn, *Mechanics of Materials 1–2: An Introduction to the Mechanics of Elastic and Plastic Deformation of Solids and Structural Materials*, 3rd edition, Printed and Bound in Great Britain by Scotprint, Musselburgh (1997).

[8] F. Beer, E. Russell, J. T. Dewolf, and D. F. Mazurek, *Mechanics of Materials*, 5th edition, Published by McGraw-Hill, New York, NY 10020 (2009).

[9] P. Obreshkov, *Woodworking Machines*, Publishing House “BM” (1995).

[10] B. Marinov, Deformation Checks in the Transmissions of Certain Classes of Woodworking Machines, *International Journal of Research in Mechanical Engineering* (2015) **3** (5), 28–41.

[11] Zh. Gochev, *Handbook for Exercise of Wood Cutting and Woodworking Tools*, (2005), Publishing House in LTU.

[12] B. Cheshankov, *Theory of Vibrations*, Publishing House of Technical University (1992).

[13] A. Pisarev, *Mechanical Vibrations*, State Publishing House Technique (1985).

[14] Š. Barcík, Experimental cutting on the table band-sawing mashine, *European Journal of Wood and Wood Products* (2003) **61** (4) 313–320, online: https://doi.org/10.1007/s00107-002-0342-9.

[15] R. Bruce, *Understanding Wood: A Craftsman's Guide to Wood Technology* Newtown, Connecticut, Taunton Press (1995).

[16] M. Yan, *Journal of Forestry Machinery & Woodworking Equipment* (1998) **8** 4–8.

[17] P. Gendraud, J. C. Roux, and J. M. Berghau, *Journal of Materials Processing Technology* (2003) **135** 109–116.

[18] R. Okai, S. Kimura, and H. Yokochi, *Journal of the Japan Wood Research Society* (1996) **42** 333–342.

[19] Y. Tonchev, *Matlab*, Part 1, State Publishing House "Technique" (2005).

[20] Y. Tonchev, *Matlab*, Part 3, State Publishing House "Technique" (2009).

Received November 15, 2024